

Length Estimation of Pneumatic Artificial Muscles for Stretch Reflex of Musculoskeletal Robots*

Mizuki Yoshida**, Wang Junqi** and Koh Hosoda**

Abstract—This paper introduces an experimental model designed to estimate the length of a pneumatic artificial muscle (PAM) from pressure and force. We model the PAM as a nonlinear spring with a spring constant dependent on deformation and pressure. The model structure has physical bases in prior research, and its coefficients are derived from static loading experiments that measure pressure, force, and length. We apply this model to estimate the length of four distinct PAMs, each varying in materials and shapes. When used in an antagonistic-muscles-driven arm, the model turned out to be effective in monitoring changes in PAM length velocity and triggering a stretch reflex, enhancing the robot’s adaptability to disturbances. The model offers a practical alternative to length sensors, contributing to greater flexibility in robot design.

I. INTRODUCTION

Soft robots are expected to achieve adaptability to environments like living organisms [1]. Soft robots that coexist with humans have been already realized [2], [3] and have been used to understand biological intelligence through a constructive methodology [4], [5]. As actuators in musculoskeletal robots, pneumatic artificial muscles (PAMs) are often used [6]. PAMs have several advantages over conventional actuators, such as a superior power-to-mass ratio [7], high compliance [8], and low cost and ease of production [9]. However, PAMs have nonlinearity because they consist of elastic materials, which places heavy computational demands on a central control system.

To overcome this hurdle, it is proposed to integrate reflex mechanisms found in living organisms into musculoskeletal robots [10]. Reflex mechanisms enable local control systems to swiftly respond to environmental changes without commands from a central control system, thereby reducing its computational load.

One of the reflex mechanisms, the stretch reflex, requires muscle length information [11], but directly measuring PAM length with a sensor poses several challenges [12]. Firstly, as a reflex action occurs instantaneously, it might lead to significant problems such as slackness in a wire encoder and light screen in a laser sensor, which could prevent accurate measurement of the PAM’s length. Secondly, because a length sensor needs to be posed at both PAM’s ends, it could

limit robot design. Thirdly, sensor stiffness might reduce the PAM’s flexibility.

This paper presents a method to estimate the PAM length from its pressure and force instead of directly measuring it with the goal of incorporating the stretch reflex into musculoskeletal robots. The proposed model views a PAM as a nonlinear spring, with the spring constant dependent on its pressure. We determined the degrees of the spring constant based on prior models and calculated its coefficients experimentally. The effectiveness of the model was demonstrated by evaluating the error in length estimation when pressure varied sinusoidally. Then the model was incorporated to the stretch reflex mechanism to maintain a robot arm in a fixed position while the falling mass generated oscillation. Applying our model allows the sensors to gather at one end of a PAM, simplifying the musculoskeletal robot design. While theoretical models of the PAM cannot accurately reflect individual differences in properties because they require almost immeasurable parameters such as fiber length and the braiding angle of the sleeve [13], our experimental approach calculates coefficients for each PAM, gaining comprehensive applicability to PAMs of various materials and shapes.

II. MODEL FOR LENGTH ESTIMATION

Regarding a PAM as a spring [14], its length is expressed as the sum of a natural length and a deformation

$$l = l_n + d \quad (1)$$

where l is the PAM length, l_n is the natural length, defined as the length without external force at pressure p , and d is the deformation from the natural length, respectively.

Assuming that l_n is a linear function of p within a certain pressure range, it can be given as

$$l_n = mp + h \quad (2)$$

where m and h can be determined by a static loading experiment.

Introducing the PAM’s nonlinearity into the spring and assuming that the spring constant is the function of p [14], the force f is given by

$$f = (a_3pd + a_2p + a_1d + a_0)d \quad (3)$$

The terms pd^2 and d^2 can be found in Chou et al.’s fundamental model [15], which capture the essential dynamic properties of the PAM. The term pd comes from Tondu et al.’s model [16] to more accurately reflect differences in the shape of the PAM. The term d is added based on Ferraresi et al.’s model [17] to account for differences in material.

*This work was supported by JSPS KAKENHI Grant Number JP23K18494

**Mizuki Yoshida, Wang Junqi and Koh Hosoda are with Department of Mechanical Engineering and Science, Graduate School of Engineering, Kyoto University, Kyoto, Japan email:yoshida.mizuki.68s@st.kyoto-u.ac.jp, wang.junqi.77a@st.kyoto-u.ac.jp, hosoda.koh.7p@kyoto-u.ac.jp

The constants $a_0 \sim a_3$ in Eq. (3) are determined by the static loading experiment. Based on the $a_0 \sim a_3$, d can be calculated from the measured p and f by solving Eq. (3).

III. EXPERIMENTAL METHOD

A. Parameter Identification

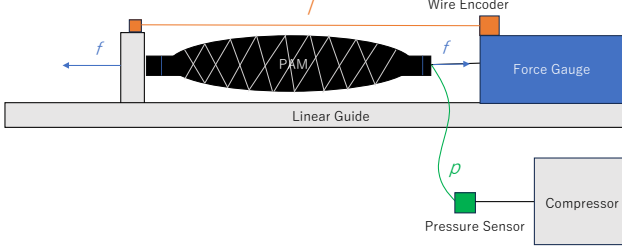


Fig. 1: Outline Diagram of Static Loading Experiment

Fig. 1 is an outline diagram of the static loading experiment to identify the parameters m , h , and a_i . Table I shows the shapes and materials of the used four PAMs. The experimental procedure was as follows. First, the pressure p was adjusted to a constant level. Taking into account the strength of the materials, the pressure of PAM-A, PAM-B, or PAM-C was adjusted to 0.4MPa, 0.5MPa, 0.6MPa, 0.7MPa or 0.8MPa, while the pressure of PAM-D was 0.2MPa, 0.3MPa, 0.4MPa, 0.5MPa, or 0.6MPa. Next, the PAM was gradually stretched from the natural length by y 2.5mm increments and the deformation d , the force f , and the pressure p were measured at each point. Each value was stabilized by waiting for at least 2 seconds after deformation. Once d reached its maximum value predetermined based on each PAM's strength, it was contracted to the natural length l_n by 2.5mm decrements, and d , p , and f were measured again at each point. Finally, the parameters m , h , and a_i were calculated by the least squares method. The pressure sensor used was PSE540(SMC Co.), the linear encoder was DS-025(MUTOH INDUSTRIES Co. Ltd.), and the force gauge was FGP-5(Nidec Co.)

TABLE I: Characteristics of Experimented PAMs

PAM	Length [cm]	Diameter [mm]	bladder Material
A	21.6	19.9	Rubber
B	21.1	13.4	Rubber
C	14.1	13.4	Rubber
D	21.2	19.0	Silicon

B. Error Evaluation

We dynamically estimated the length of the four different PAMs to verify the general applicability of the model. The jig holding the left end of the PAM in Fig. 1 was removed and a pulley was installed in its place. A proportional control valve was installed between the pressure sensor and the compressor. The experiment procedure was as follows. First, a weight of either 5kg or 10kg was connected to the PAM via the pulley to apply a constant force f . Next, considering

the strength of each PAM, the pressure p [MPa] was varied over time t [s] by the proportional control valve according to

$$p = 0.2 \sin\left(\frac{2\pi t}{5}\right) + 0.6 \quad (4)$$

for PAM-A, PAM-B, and PAM-C, and

$$p = 0.2 \sin\left(\frac{2\pi t}{5}\right) + 0.4 \quad (5)$$

for PAM-D. At each time, f , p , and the length l were measured. Finally, the errors were calculated between the measured and estimated l .

C. Reaching Task

We conducted an reaching experiment to see the errors when the model is actually incorporated into the stretch reflex mechanism. The system developed by Takahashi et al. [10] was adapted and located in a vertical direction. The system consisted of an arm with a pair of PAMs, an agonist muscle and an antagonist muscle, and the muscles were connected to the arm with fishing line. The force gauge used in the parameter identification experiment was too big to be equipped with the robot arm, so it was replaced with a foil strain gauge (KFP-5-120-C1-65L1M2R, Kyowa Electronic Instrument Co. Ltd.). The reaching movement was performed by linearly increasing the pressure of the agonist muscle from 0.2MPa to 0.6MPa while decreasing the pressure of the antagonist muscle from 0.6MPa to 0.2MPa. During the reaching movement, the length of the PAMs was measured with the linear encoder while it was estimated by the predetermined parameters m , h , and a_i , and the errors were calculated. The experiment time was 12s, and the sampling frequency was set to

100Hz.

During the experiment, the change in resistance of the strain gauges went to a quarter Wheatstone bridge circuit where the three resistors other than the strain gauge were $120 \pm 0.5\Omega$. Unlike the force gauge, which can directly measure the force of the PAMs, the voltage signal from the circuit was converted to force according to Eq.(6). Eq.(6) assumes that the voltage is a linear function of force because the voltage from the Wheatstone bridge circuit is proportional to the strain [18] and the strain is proportional to the force while the material is elastically deformed.

$$V = qf + V_{base} \quad (6)$$

V is the voltage signal from the strain gauge, q is the slope between the voltage and the force, and V_{base} is the base voltage when no force is applied. The parameter was obtained by statically loading the PAMs and simultaneously measuring the voltage and the force. Eq.(6) can be rewritten as

$$f = \frac{1}{q} \Delta V \quad (7)$$

where $\Delta V = V - V_{base}$. Substituting Eq.(7) into Eq.(3) gives

$$\Delta V = (a'_3 p d + a'_2 p + a'_1 d + a'_0) d \quad (8)$$

where $a'_i = q a_i$, and the deformation d can be calculated by solving this equation.

D. Stretch Reflex

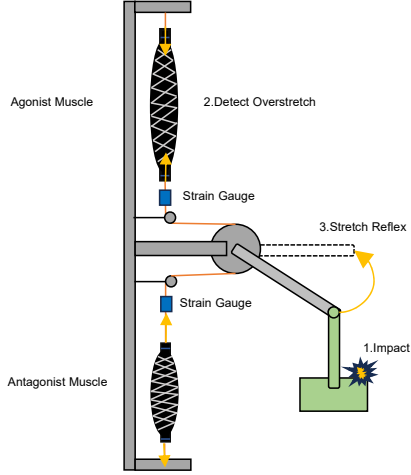


Fig. 2: Outline Diagram of Stretch Reflex Experiment

Fig. 2 is an outline diagram of the stretch reflex experiment. The arm was equipped with the basket and expected to keep it in a fixed position by maintaining the pressure of the PAMs at 0.4MPa, and a 0.5kg mass was dropped from a certain height to make an impact. During the experiment, the velocity of the PAMs was calculated as

$$v_j = \frac{l_j - l_{j-1}}{dt} \quad (9)$$

where j is the sampling number, l_j is the estimated length, and dt is the sampling period. Since the system was set to 100Hz, dt was 0.01s. When the impact rapidly stretched the agonist PAM and its velocity exceeded a predetermined threshold, the stretch reflex was induced. The pressure command from the stretch reflex controller converged to the goal pressure from a top controller as follow:

$$p_{ago} = p_{tp-ago} + \Delta p_{ago-exci} - \Delta p_{anta-inhi} \quad (10)$$

$$p_{anta} = p_{tp-anta} + \Delta p_{anta-exci} - \Delta p_{ago-inhi} \quad (11)$$

where p_{tp} is the goal pressure from the top controller, Δp_{exci} is the excitatory pressure, and Δp_{inhi} is the reciprocal inhibition pressure. Δp_{exci} and Δp_{inhi} were calculated by the following equations:

$$\Delta p_{exci} = \Delta p_{inhi} = kv \quad (12)$$

where k is the gain determined experimentally. Takahashi et al. designed this command process inspired by α motor neurons located in human spinal cords [10]. The positioning task was performed with and without the stretch reflex, and the reaction speeds were compared.

IV. RESULT

A. Parameter Identification

Fig. 3 shows the relationship between the pressure p and the natural length l_n of the PAMs. As assumed, there is a tendency for l_n to decrease linearly with p within the range of the tested pressure. The dashed lines in Fig. 3 represent

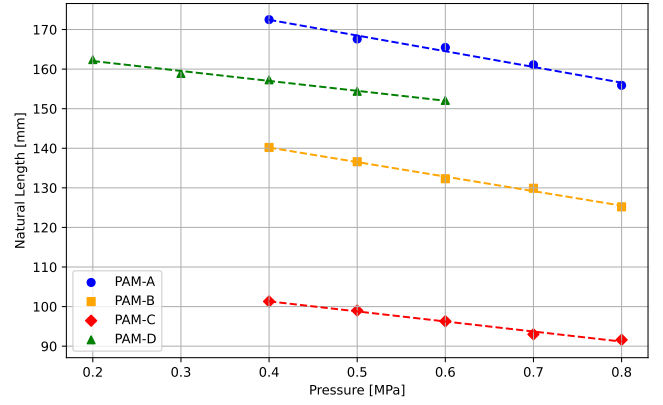


Fig. 3: Relationship between Pressure and Natural Length

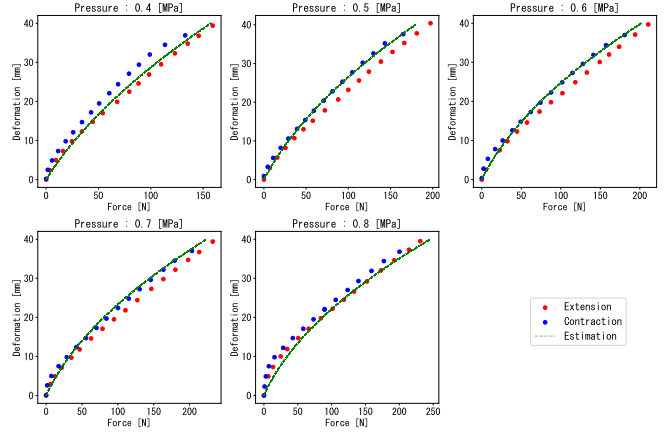


Fig. 4: Relationship between Force and Deformation at Each Pressure (PAM-B)

the fitted lines using the least squares method, expressed by Eq. (2).

Fig. 4 shows the result of the static loading experiment for PAM-B. The red and blue points represent the data during expansion and contraction respectively, and the green dashed lines represent the solutions d to Eq. (3), which is given by substituting the acquired parameters a_i and the measured f and p . Generally, PAMs exhibit hysteresis due to friction, so the data differ between expansion and contraction processes. We only present the static loading experimental result for PAM-B because of the space constraint, but similar results were obtained for the other PAMs.

B. Error Evaluation

Fig. 5 and Fig. 6 show the dynamic length estimation result for PAM-B and PAM-D, respectively. With the proposed method, the length estimation was achieved with maximum errors of 1.72% for PAM-A, 1.19% for PAM-B, 1.18% for PAM-B, and 1.65% for PAM-D respectively, and with mean squared errors of 0.861% for PAM-A, 0.653% for PAM-B, 0.683% for PAM-C, and 0.846% for PAM-D respectively.

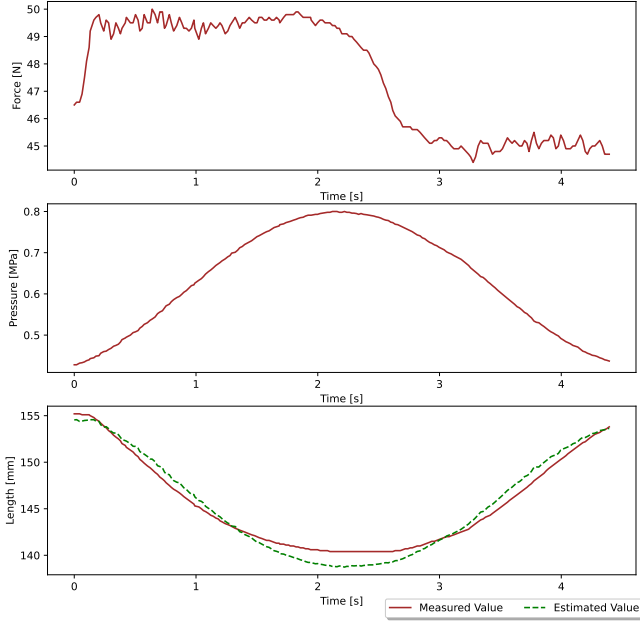


Fig. 5: Dynamic Length Estimation (PAM-B, Rubber)

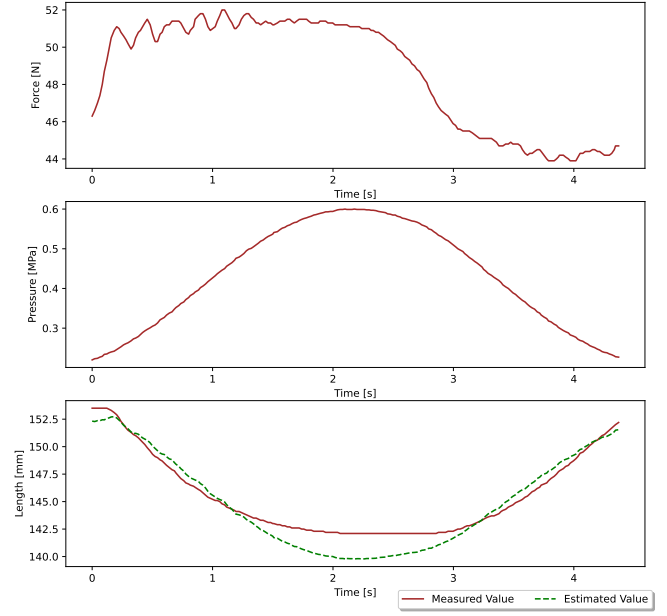


Fig. 6: Dynamic Length Estimation (PAM-D, Silicon)

C. Reaching Task

Table. II shows the parameters for the length estimation of the agonist and antagonist muscles. The considerable difference in the voltage-force slope q between the two PAMs is attributable to the varying sensitivities of the handmade force gauges.

TABLE II: Parameters for Length Estimation

PAM	m	h	a_3	a_2	a_1	a_0	q
Agonist	-60.1	170.1	-0.201	7.00	0.256	0.911	1.84
Antagonist	-70.3	178.5	0.871	1.24	-0.129	22.4	3.55

D. Stretch Reflex with Model

Table III shows the velocity threshold V_{thr} , which were determined by assessing the magnitude of the impact in advance.

TABLE III: Parameters for Stretch Reflex

PAM	V_{thr}	k
Agonist		
Antagonist		

V. DISCUSSION

To improve length estimation accuracy, we expanded Eq. (3) by adding the terms p^2 and d^2 and increasing the parameters as follows:

$$F = (b_5 p^2 + b_4 p d + b_3 d^2 + b_2 p + b_1 d + b_0) d \quad (13)$$

As a result, the dynamic length estimation was achieved with the maximum errors of 1.12% for PAM-A, 0.773% for PAM-B, 1.01% for PAM-B, and 0.755% for PAM-D respectively,

and with the root mean squared errors of 0.633% for PAM-A, 0.353% for PAM-B, 0.548% for PAM-C, and 0.435% for PAM-D respectively. The errors were reduced as expected for all PAMs.

We also tried another approach by introducing a cubic polynomial model and increasing the parameters as follows:

$$F = (c_4 p^3 + c_3 p^2 d + c_2 p d^2 + c_1 d^2 + c_0) d \quad (14)$$

As predicted, the root mean squared errors decreased to 0.516% for PAM-A, 0.484% for PAM-B, 0.500% for PAM-C, and 0.606% for PAM-D respectively. However, even though the maximum errors decreased to 1.22% for PAM-A and 0.951% for PAM-C respectively, they actually increased to 1.41% for PAM-B and 1.99% for PAM-D respectively. This result suggests that, even if the coefficients of the model equation are determined experimentally, the degrees must be carefully determined based on previous studies so as to express intrinsic characteristics of the PAM. For example, the newly added term p^3 may have amplified the error of the pressure sensor. When applying our model to a reflex mechanism, it will also be necessary to carefully consider the contribution of each term to the accuracy of the length estimation based on the reliability of the force and pressure sensors used.

Wickramatunge et al. proposed separating the parameters a_i into contraction ones a_i^c and extension ones a_i^e to reflect the hysteresis of the PAM [14]. They also suggested using different parameters for low-pressure and high-pressure ranges to further improve the accuracy. However, our model ignores these suggestions and simplifies the length estimation method by using the same parameters across the entire pressure range, regardless of contraction or expansion. This is because our model is supposed to be applied to the reflex

mechanism. If the parameters have to be switched depending on the situation, it would be difficult for the reflex mechanism to respond quickly to disturbances. Musculoskeletal robots often carry microcomputers on their structures, so the employed length estimation method is desired to be simple for efficient operation given the limited computational resources.

REFERENCES

- [1] D. Rus and M. T. Tolley, "Design, Fabrication and Control of Soft Robots," *Nature*, vol. 521, pp. 467–475, 2015.
- [2] H. Sato, K. Uchiyama, Y. Mano, F. Ito, S. Kurumaya, M. Okui, Y. Yamada, and T. Nakamura, "Development of a Compact Pneumatic Valve Using Rotational Motion for a Pneumatically Driven Mobile Robot With Periodic Motion in a Pipe," *IEEE Access*, vol. 9, pp. 165271–165285, 2021.
- [3] P. Polygerinos, Z. Wang, K. C. Galloway, R. J. Wood, and C. J. Walsh, "Soft Robotic Glove for Combined Assistance and At-Home Rehabilitation," *Robotics and Autonomous Systems*, vol. 73, pp. 135–143, 2015.
- [4] K. Hosoda, S. Sekimoto, Y. Nishigori, S. Takamuku, and S. Ikemoto, "Anthropomorphic Muscular–Skeletal Robotic Upper Limb for Understanding Embodied Intelligence," *Advanced Robotics*, vol. 26, no. 7, pp. 729–744, 2012.
- [5] A. D. Marchese, C. D. Onal, and D. Rus, "Autonomous Soft Robotic Fish Capable of Escape Maneuvers Using Fluidic Elastomer Actuators," *Soft Robotics*, vol. 1, no. 1, pp. 75–87, Mar. 2014.
- [6] S. M. Mirvakili and I. W. Hunter, "Artificial Muscles: Mechanisms, Applications, and Challenges," *Advanced Materials*, vol. 30, no. 6, 2018.
- [7] D. B. Reynolds, D. W. Repperger, C. A. Phillips, and G. Bandry, "Modeling the Dynamic Characteristics of Pneumatic Muscle," *Annals of Biomedical Engineering*, vol. 31, no. 3, pp. 310–317, 2003.
- [8] C.-P. Chou and B. Hannaford, "Static and Dynamic Characteristics of McKibben Pneumatic Artificial Muscles," in *Proceedings of the 1994 IEEE International Conference on Robotics and Automation*, pp. 281–286, IEEE Comput. Soc. Press, 1994.
- [9] K. P. Ashwin and A. Ghosal, "A Survey on Static Modeling of Miniaturized Pneumatic Artificial Muscles With New Model and Experimental Results," *Applied Mechanics Reviews*, vol. 70, no. 4, 2018.
- [10] R. Takahashi, Y. Wang, J. Wang, Y. Jiang, and K. Hosoda, "Implementation of Basic Reflex Functions on Musculoskeletal Robots Driven by Pneumatic Artificial Muscles," *IEEE Robotics and Automation Letters*, vol. 8, no. 4, pp. 1920–1926, 2023.
- [11] E. R. Kandel, J. H. Schwartz, T. M. Jessell, S. Siegelbaum, A. J. Hudspeth, S. Mack et al., *Principles of Neural Science*. McGraw-Hill, New York, 2000, vol. 4.
- [12] R. Sakurai, M. Nishida, H. Sakurai, Y. Wakao, N. Akashi, Y. Kuniyoshi, Y. Minami, and K. Nakajima, "Emulating a Sensor Using Soft Material Dynamics: A Reservoir Computing Approach to Pneumatic Artificial Muscle," in *2020 3rd IEEE International Conference on Soft Robotics (RoboSoft)*, pp. 710–717, 2020.
- [13] T. Nozaki and T. Noritsugu, "Motion Analysis of McKibben Type Pneumatic Rubber Artificial Muscle with Finite Element Method," *International Journal of Automation Technology*, vol. 8, pp. 147–158, 2014.
- [14] K. C. Wickramatunge and T. Leephakpreeda, "Empirical Modeling of Dynamic Behaviors of Pneumatic Artificial Muscle Actuators," *ISA Transactions*, vol. 52, no. 6, pp. 825–834, 2013.
- [15] C.-P. Chou and B. Hannaford, "Measurement and Modeling of McKibben Pneumatic Artificial Muscles," *IEEE Transactions on Robotics and Automation*, vol. 12, no. 1, pp. 90–102, 1996.
- [16] B. Tondu and P. Lopez, "Modeling and Control of McKibben Artificial Muscle Robot Actuators," *IEEE Control Systems*, vol. 20, no. 2, pp. 15–38, 2000.
- [17] W. F. Carlo Ferraresi and A. Manuello, "Flexible Pneumatic Actuators: A Comparison between The McKibben and the Straight Fibres Muscles," *Journal of Robotics and Mechatronics*, vol. 13, no. 1, pp. 56–63, 2001.
- [18] K. Hoffmann, "Applying the Wheatstone Bridge Circuit," HMB Germany, 1974.